termined in the dark at each humidity level. The values were used as estimates of surface-adsorbed pollutant flux in the light and were subtracted from total pollutant flux in the light to calculate uptake into plant leaves.
15. A. C. Hill and N. Littlefield, *Environ. Sci. Technol.* 1, 52 (1969).
16. S. Rich and N. C. Turner, *J. Air Pollut. Control Assoc.* 22, 718 (1972).
17. M. Mansfield and O. Majernik, *Environ. Pollut.* 3, 1 (1970).
18. J. Bonte and P. Louguet, *Physiol. Veg.* 13, 1 (1970).
19. A. C. Chamberlain, in *Air Pollutants and Their Effects on the Terrestrial Ecosystem*, S. V. Krupa and A. H. Legge, Eds. (Wiley-Interscience, New York, in press).
20. Leaf resistance is comprised of a gas-phase resistance and a series of liquid-phase (residual) resistances between initial absorption of the pollutant in the water on mesophyll walls and its initial biochemical reactions. These residual resistances are collectively referred to as mesophyll resistance. Changes in mesophyll resistance calculated by the Ohm's law formula may also be caused by internal factors that alter the leaf concentration of the gas in question and the air-leaf concentration gradient. Separation of resistance and gradient-induced changes in uptake is not generally attempted and not within the scope of this report.
21. D. S. Shriner *et al.*, *Oak Ridge Natl. Lab. Rep. ORNL/TM-5919* (1977).
22. Research sponsored by the U.S. Environmental Protection Agency under interagency agreement 40-740-78 and by the U.S. Department of Energy under contract W-7405-eng-26 with Union Carbide Corporation. Publication 1629, Environmental Sciences Division, Oak Ridge National Laboratory.

30 July 1980; revised 17 October 1980

Phosphorus Distribution in the Nucleosome

Abstract. *The spatial distribution of phosphorus within active fraction nucleosomes reveals that the path of the DNA is consistent with one and three-fourths turns of DNA supercoiled around the outside of the protein core. This phosphorus distribution, obtained with an imaging electron spectrometer in a conventional transmission electron microscope, simultaneously establishes new limits of sensitivity for elemental microanalysis.*

We have adapted a high-resolution electron microscope with an imaging electron energy spectrometer capable of resolving structural information of biological specimens to at least the 0.5-nm level while supplying chemical information with the same spatial resolution (*1*). The electron spectrometer allows an electron micrograph to be formed by using electrons that have lost a discrete amount of energy as a result of interactions with a particular chemical element or chromophore in the specimen. We have used this instrument to study the DNA distribution in the subunits of eukaryotic chromatin known as nucleosomes. We are able to locate the path of the DNA within the nucleosome and between nucleosomes by electron spectroscopic imaging that makes use of an energy loss due to phosphorus. Since phosphorus is primarily found in the DNA and not in the proteins constituting the particle, an image of the phosphorus distribution is predominantly an image of the DNA within the nucleosome.

The chromatin was prepared from calf thymus and enriched for active fraction chromatin by deoxyribonuclease II digestion and Mg^{2+} solubility (*2*). The buffer containing the chromatin was adjusted to 0.35*M* NaCl to remove the high-mobility group (HMG) proteins. The oligomers of nucleosomes were then separated from the free proteins by chromatography (Sepharose 4B, Pharmacia). Microscope grids of unstained chromatin were prepared as described (*3*), and micrographs were obtained with axial illumination at the desired energy loss, a dose of about 1.4 coulombs per square centimeter being used to form each image.

Electrons interacting with phosphorus have characteristic energy losses corresponding to K-shell and L-shell excitations of the phosphorus atoms. We have used the relatively strong $L_{2,3}$ excitations at 132 eV. In the electron energy loss spectrum, this specific phosphorus L-edge absorption is superimposed on a rapidly declining general background of localized and delocalized electron-scattering events. The effect of this background signal was eliminated by forming two consecutive images of the same region, one on the phosphorus L edge and one with an energy just below the edge. The latter image, normalized in intensity, must then be subtracted from the former to obtain a net phosphorus signal.

Figure 1 shows two images of the same strand of nucleosomes. One image (Fig. 1a) was formed at an energy loss of 155 eV, just above the L edge at 132 eV, referred to as the phosphorus spectroscopic image, and the other (reference) image (Fig. 1b) at an energy loss of 105 eV. The two images are nearly identical. However, close examination shows fine structural detail in one image that is not always duplicated in the other. The two images were digitized with a microdensitometer (Perkin-Elmer model 1010A) over regions containing the nucleosomes to give matrices of 4096 picture elements (64 × 64), each corresponding to 0.7 by 0.7 nm^2. Although the potential resolution of electron spectroscopic images is at least 0.7 nm (*1*), digitization with this pixel size limits the effective resolution of the images to 1.4 nm at worst. However, this is still sufficient for a DNA strand that is approximately 2 nm in thickness to be visualized. Before the subtraction was performed, one image was normalized to the other over the background to compensate for slightly different exposures. In addition, corresponding pairs of images were translationally cross-correlated in the computer to obtain the best overlap. Rotational cross-correlation was not necessary since consecutive images were sufficiently parallel.

We have studied 30 nucleosomes from one chromatin strand in detail, the first 13 of which are shown in Fig. 1 and the last 7 in Fig. 2a. In Fig. 2b, the computer-processed net phosphorus images have been superposed over the corresponding nucleosomes in the original phosphorus spectroscopic image. Al-

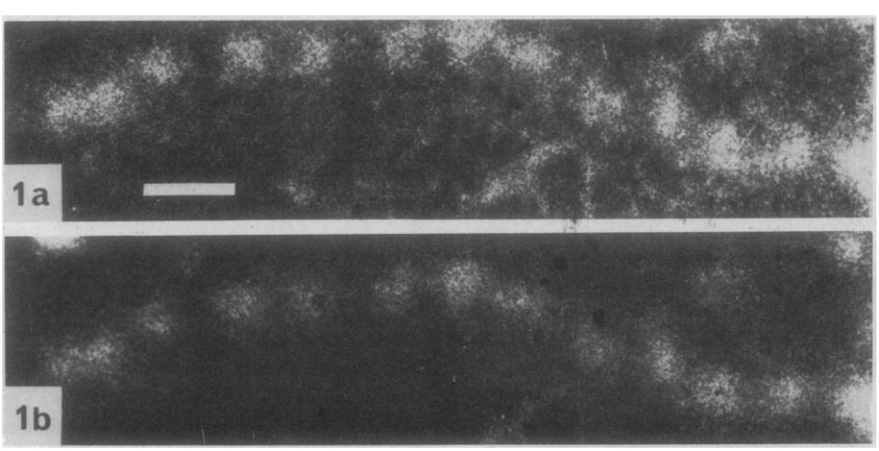

Fig. 1. (a) Phosphorus spectroscopic image of a strand of nucleosomes taken at an energy loss of 155 eV, just above the $L_{2,3}$ absorption edge of phosphorus. (b) Reference image of the same region shown in (a), taken at an energy loss of 105 eV. Scale bar, 30 nm.

0036-8075/81/0109-0169$00.50/0

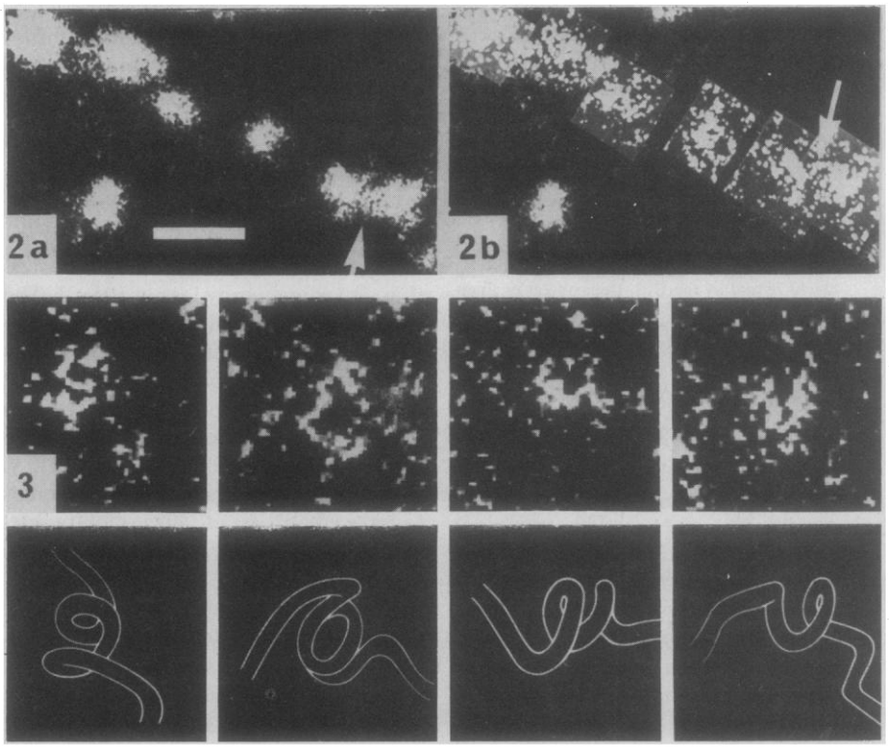

Fig. 2. (a) Phosphorus spectroscopic image of a strand of nucleosomes. The arrow indicates a region between two nucleosomes where we might expect the DNA to link the particles. (b) Computer-processed net phosphorus images of the same region as (a), superimposed over a copy of (a). The contrast is greater in the net phosphorus images because the optical density scale has been expanded. The arrow shows where the linker DNA is located. Relatively little phosphorus exists in the region indicated by the arrow in (a). Scale bar, 30 nm. Fig. 3. Net phosphorus images of four nucleosomes with artist's freehand interpretations of DNA coiling below. Full size is 38.5 nm.

though the net signal is smaller, the contrast is far greater in the net phosphorus images, because the optical density scale has been expanded. The concentrations of phosphorus over the nucleosome images stand out clearly. In most instances, even the phosphorus in the DNA linking the nucleosomes can be discerned. The net phosphorus image is sometimes essential in determining the location of the linker DNA. For instance, the arrow in Fig. 2a indicates a region between two adjacent nucleosomes where we might expect the DNA to link the particles. However, the net phosphorus image illustrates that this region contains no phosphorus and that, instead, the linking DNA is just above this region, as indicated by the arrow in Fig. 2b.

Knowledge of the track of the linker DNA aided greatly in the interpretation of the coiling of the DNA within the core particle. The phosphorus distribution within 22 of the 30 consecutive nucleosomes examined in detail could be readily interpreted as being consistent with the model for the core particle of Finch *et al.* (*4*), who proposed that $1^3/_4$ turns of DNA are found in a single nucleosome. In the other eight nucleosomes, the phosphorus signal was still very strong, but the spatial distribution did not follow the simple superhelical configuration. This could result from radiation-induced alterations or may be real temporary conformational changes at these sites due to transcription. Figure 3 shows four of the 22 net phosphorus images along with corresponding artist's interpretations of DNA coiling based on the current model.

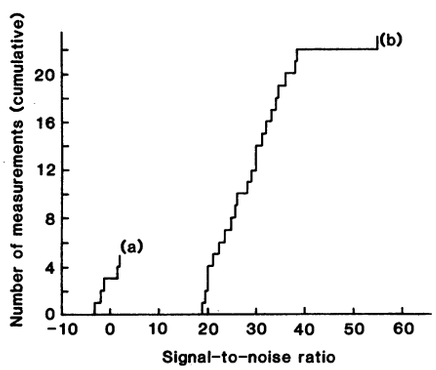

Fig. 4. (a) Cumulative histogram of signal-to-noise ratios in the subtracted images of two consecutive dark-field micrographs calculated over the region of individual nucleosomes. (b) Histogram of signal-to-noise ratios of the net phosphorus images, calculated over the regions of individual nucleosomes.

The possibility of radiation-induced structural alterations must be examined. The phosphorus distribution in the nucleosome is obtained by subjecting the sample to very high radiation. The problem is compounded because the subtraction of two images is necessary to obtain a net phosphorus signal. To determine whether the net phosphorus image could be artifactual, we formed two consecutive dark-field electron micrographs of nucleosomes in a previously unirradiated region. The total dose to the specimen was the same as that required to form the phosphorus spectroscopic and the reference images. The signal-to-noise ratio in the difference images in these control experiments over the regions of the nucleosomes for five different image pairs was -0.78 ± 1.01 (standard error). However, the average signal-to-noise ratio calculated over the region of the nucleosomes in the net phosphorus images was 29.1 ± 1.7 (Fig. 4). Thus there is no question that the phosphorus signal observed is real. The signal comes from 140 base pairs of DNA, or 280 atoms of phosphorus. If a signal-to-noise ratio as low as 5 were considered to be the limit of certain detection (*5*), it would still be possible, with this technique, to detect 48 phosphorus atoms or 2.5×10^{-21} g of phosphorus.

Our results illustrate the usefulness of electron spectroscopic imaging for obtaining structural and chemical information simultaneously with fairly high resolution. The application of this technique to the nucleosome has demonstrated that the model of DNA coiling proposed for these particles is consistent with the phosphorus distribution within nucleosomes from the transcriptionally competent fraction.

D. P. BAZETT-JONES
F. P. OTTENSMEYER
Department of Medical Biophysics, University of Toronto, and *Physics Division, Ontario Cancer Institute, Toronto, Canada M4X 1K9*

References and Notes

1. F. P. Ottensmeyer and J. W. Andrew, in preparation.
2. J. M. Gottesfeld and P. J. G. Butler, *Nucleic Acids Res.* **4**, 3155 (1977).
3. F. P. Ottensmeyer, R. F. Whiting, E. E. Schmidt, R. S. Clemens, *J. Ultrastruct. Res.* **52**, 193 (1975).
4. J. T. Finch, L. C. Lutter, D. Rhodes, R. S. Brown, B. Rushton, M. Levitt, A. Klug, *Nature (London)* **269**, 29 (1977).
5. A. Rose, *Vision: Human and Electronic* (Plenum, New York, 1973), p. 14.
6. We thank E. Macpherson for technical assistance. Supported by grants from the National Cancer Institute of Canada, grant MA 37-63 from the Medical Research Council of Canada, and a grant from the Ontario Cancer Treatment and Research Foundation. D.P.B.-J. holds a research studentship from the National Cancer Institute.

23 April 1980